Large Diurnal Sea Surface Temperature Variability: Satellite and In Situ Measurements*

LOTHAR STRAMMA AND PETER CORNILLON

Graduate School of Oceanography, University of Rhode Island, Kingston, RI 02881

ROBERT A. WELLER, JAMES F. PRICE AND MELBOURNE G. BRISCOE

Woods Hole Oceanographic Institution, Woods Hole, MA 02543

(Manuscript received 29 April 1985, in final form 18 October 1985)

ABSTRACT

Data from a surface mooring located in the Sargasso Sea at 34°N, 70°W between May 1982 and May 1984 were compared with satellite data to investigate large diurnal sea surface temperature changes. Mooring and satellite measurements are in excellent agreement for those days on which no clouds covered the site at the time of the satellite pass. During the summer half-year at this site, there is a 20% chance of diurnal warming of more than 0.5°C, with values of up to 3.5°C observed in the two-year period.

Diurnal warming observed at the mooring has been simulated well by a one-dimensional model driven by local heat and momentum fluxes. Under the conditions of very light wind and strong insolation that produce the largest surface warming, the surface mixed-layer depth reduces to the convection depth, and wind-mixing becomes unimportant. The thermal response is then limited to depths between 1 and 2 m, making it likely that such events have been underreported in routine ship observations.

In all cases observed, the spatial extent of warming events as determined by satellite data are well correlated with the corresponding atmospheric pressure patterns. Conditions giving rise to the largest diurnal warming events are often associated with a westward-extending ridge of the Bermuda high. In the region studied, 57°–75°W and 29°–43°N, diurnal warming of more than 1°C was found on occasion to cover areas in excess of 300 000 km^2, with warming of more than 2°C covering areas in excess of 130 000 km^2.

1. Introduction

The thermal boundary layer between the ocean and the atmosphere has received significant attention in recent years because of interest in sea surface temperature (SST) as a predictor of large-scale, long-range changes in weather patterns. Therefore, a complete understanding of the processes in the boundary layer and the exchange between the atmosphere and the ocean is necessary. It is thought that large day-to-day fluctuations in SST, depth of the thermocline and stored heat may result from variations in wind and solar insolation. Stommel et al. (1969) presented observations of diurnal temperature changes in the upper 60 m of water south of Bermuda in March 1968. Nine diurnal cycles under differing conditions of wind and cloud cover showed SST variations of 0.1 to 1.0°C. In the Bermuda area in August 1974, on a day with low winds, Kaiser (1978) observed a layer of 3.9 m depth which was over 1°C warmer than the water below. In the MODE experiment southwest of Bermuda, Bruce and Firing (1974) observed under light winds (2–4 m s^{-1}) a shallow 1–2 m layer that was 2–3°C warmer than the main mixed layer. In the eastern Atlantic, Halpern and Reed (1976) found diurnal warming of up to 1.4°C in March 1972 at 21°40′N near the African coast. Despite these few studies, the overall scarcity of observations of large diurnal warming has fostered the assumption that diurnal temperature variations at the surface in the open ocean are small. Furthermore, because the few observations made to date were from ships, they cover only a few days at isolated locations. Thus, little knowledge exists about horizontal scales or statistics of SST fluctuations due to diurnal warming.

Horizontal scales may be computed from satellite observations. Deschamps and Frouin (1984) used satellite data to show diurnal warming in the Mediterranean Sea. Unfortunately they had no in situ data with which to verify their observations. Lynn and Svejkovsky (1984) examined changes in surface temperature both from satellite and ship data in the eastern North Pacific over a two-day interval in late November. Their in situ temperature measurements at 1 m depth suggest a diurnal variation of 0.2°C, much less than the 0.25 to 1.0°C variation which they observed by satellite.

During a two-year period from May 1982 to May 1984, a Woods Hole Oceanographic Institution mooring was deployed at 34°N, 70°W for the Long Term Upper Ocean Study (LOTUS; Briscoe and Weller, 1984) to obtain a description of the response of the

* Woods Hole Oceanographic Institution Contribution No. 5953.

upper ocean to atmospheric forcing. During the same period all of the satellite data from the TIROS-N series Advanced Very High Resolution Radiometers (AVHRR) were acquired. In this study, the satellite observations, the LOTUS mooring data and the output from a one-dimensional model of the surface mixed layer are compared for days on which significant diurnal warming was observed at the LOTUS thermistor. Following these comparisons, designed to validate the satellite data as well as address the physics of such warming events, the spatial distribution of warming events is correlated with synoptic weather patterns.

2. Mooring measurements

The LOTUS mooring consisted of a 3.5-m diameter discus buoy carrying meteorological instruments as well as near-surface temperature sensors and current meters. It was deployed in May 1982, replaced every six months and recovered in May 1984. Several gaps exist in the surface data but these had no effect on this investigation because they all occurred in the winter months (from late October through early April of either 1982–83 or 1983–84). Large diurnal SST differences at the LOTUS position occur only between the end of April and the beginning of October. The mooring was taut, with a scope of close to 1, and the buoy stayed within 10° of vertical even in 3 m seas. A more complete description of the buoy and the meteorological and oceanographic sensors is given in Deser et al. (1983).

The meteorological recorder was a Vector Averaging Current Meter (VACM) converted for use as a Vector Averaging Wind Recorder (VAWR; Payne, 1974). Two redundant VAWRs were mounted on the LOTUS buoy for the May–October 1982 deployment, and a third set of meteorological sensors telemetered data via the Argos satellite. The VAWRs both had cup and vane wind sensors and thermistor air temperature sensors, one with a Thaller shield and the other with a PRL shield. Also attached to the VAWRs was a sea temperature thermistor fixed 0.6 m below the water line of the buoy, an Eppley pyranometer and a Digiquartz barometric pressure sensor. The third sensor package provided additional measurements of wind, air temperature and barometric pressure. The three datasets were compared to verify the performance of the sensors and to identify and eliminate data from sensors that had failed or degraded. Based on this comparison, the accuracy of the measured wind speed was within 10%. The air temperature data from the sensor in the Thaller shield was used because the record from the sensor with the PRL shield showed a diurnal fluctuation associated with direct radiative heating; the sensors themselves were accurate to 0.01°C. When the ocean was well mixed, the sea temperature data from 0.6 m agreed well with the temperature data from the current meter at 5 m; the accuracy of the sea temperature measurement was 0.01°C. Current meters located at 5, 10, 15 and 25 m and deeper depths on the mooring line beneath the buoy provided a record (0.01°C accuracy) of the temperature structure in the upper ocean. VAWR measurements of relative humidity were unusable, because of suspected contamination of the sensor by salt.

During the summer of 1983, data on wind velocity, sea temperature at 0.6 m, air temperature, solar radiation and barometric pressure were collected from a single VAWR. Redundancy of meteorological observations was provided by additional meteorological packages. Accuracies of the 1983 data are similar to those of the 1982 data.

3. Satellite measurements

Retrievals of SST using the split window approach have been shown to be superior to those using a single spectral channel or a pair of windows in separate spectral regions (McMillin and Crosby, 1984). For this reason only data obtained from the NOAA-7 borne AVHRR (Schwalb, 1978) have been used in this study. Values of SST were obtained from the following equation:

$$T_{ss} = \alpha_0 + \alpha_1 T_{11} + \alpha_2 (T_{12} - T_{11}), \qquad (1)$$

where T_{ss} is the desired SST value, T_{11} is the channel 4 brightness temperature, T_{12} is the channel 5 brightness temperature, and α_0, α_1 and α_2 are regression coefficients. NOAA/NESDIS (1982) determined the values of these coefficients (presented in Table 1) by regressing the channel 5 brightness temperature and the channel 4 and 5 brightness temperature difference on the buoy-derived SST, using match-ups from drifting buoys in the North and South Atlantic, the northeastern and tropical North Pacific, the subtropical and midlatitude South Pacific, and the Indian Ocean. The NESDIS group defined a match-up as a drifting buoy observation within 24 h and 50 km of a satellite pass. The regression was performed separately for nighttime and daytime observations because of a persistent negative bias in the nighttime satellite retrievals (McClain et al., 1983). Neither the 24 h interval for a match-up nor the different set of regression coefficients between day and night is a problem because most of the NESDIS observations were obtained in areas with no diurnal warming. This is apparent from the fact that the satellite-derived SST fields used in this study showed the same temperature for daytime and nighttime passes outside of warming events.

TABLE 1. Regression coefficients for the SST retrieval algorithm derived by NOAA/NESDIS.

Equation	α_0	α_1	α_2
Daytime	−283.93	1.0351	−3.046
Nighttime	−288.23	1.0529	−2.627

Interpretation of the satellite-derived SST field is complicated by the thin skin at the ocean surface from which satellite measurements are made. This skin, which is only several micrometers thick, has been shown to be as much as 0.3° to 0.6°C cooler than the temperature directly beneath (Paulson and Simpson, 1981). For low wind speeds, however, temperature differences between the cool surface skin and the layer beneath should be low. For example, Grassl (1976) found the temperature difference between the cool skin and the layer beneath to be 0.2°C for wind speeds of 1 m s^{-1}. Furthermore, solar radiation tends to compensate for cooling at the surface since the top few millimeters strongly absorb incoming radiation in daytime. Finally, the algorithm used to calculate SST from satellite data was derived by regressing in situ SST values from Eq. (1); hence, the cool skin is in part incorporated in the coefficients of this equation.

4. Satellite-mooring intercomparison

In this section satellite-derived day–night SST differences at 34°N, 70°W are compared with the corresponding differences derived from the LOTUS 0.6 m deep thermistor. The first step in this comparison involves the selection of times at which the data are to be compared. The selection procedure begins by identifying possible occurrences of diurnal warming from the LOTUS data. For the period May 1982–October 1983, temperature observations for which the maximum daytime temperature exceeded the minimum temperature of the previous night by 0.5°C were divided into 0.5°C bins. The 0.5°C threshold was selected because, as will be shown, this is the minimum temperature difference reliably detected in the satellite data. In order to avoid including occurrences for which the temperature difference exceeds the 0.5°C threshold but which result from the advection of thermal features past the mooring, an additional constraint was imposed on the event: the surface temperature was required to fall by at least 0.5°C on the following night. As can be seen in Table 2, 11% (81) of the days in the two years considered meet both of these constraints. If only the period April–October is considered, the probability increases to approximately 20%.

In the next step, data were rejected because of excessive cloud cover. First, 31 of the 81 days summarized in Table 2 were rejected prior to examining the satellite data because the LOTUS insolation record indicated heavy cloud cover. Second, of the remaining 50 days, 28 were rejected because of cloud cover detected in at least one of the two satellite passes required for a diurnal pair. A diurnal pair is defined as the daytime pass showing the event and either the previous or the following nighttime pass. Cloud contamination at LOTUS was determined subjectively by a trained analyst viewing a high-contrast display of the full-resolution satellite-derived SST field.

TABLE 2. Number of day–night pairs for which the minimum of the night–day or the day–following night temperature difference at the LOTUS mooring (0.6 m below the surface) lies within the specified range.

	Temperature (°C)					
Year	[0.5, 1.0)*	[1.0, 1.5)	[1.5, 2.0)	[2.0, 2.5)	[2.5, 3.0)	Total
1982	26	6	5	3	2	42
1983	28	9	2	—	—	39

* The notation $[x, y)$ means $\geq x$, $< y$.

In summary, of the 81 days indicating possible diurnal warming in excess of 0.5°C in the LOTUS dataset, 22 had clear satellite images at LOTUS for the previous night and the day itself, or the day and the following night. These 22 night–day or day–following night sets were made of 39 images (less than the 44 expected because of consecutive days for which the preceding night of one day was the following night of the previous day). In direct comparisons with LOTUS thermistor data, satellite SST values were averaged over a 5 × 5 pixel square centered on LOTUS. The resulting 39 SST values are, on the average, 0.05°C higher than the corresponding 0.6 m deep mooring value and, relative to these data, have a standard deviation of 0.45°C.

A four-day period of small cloud cover beginning on 14 July 1982 showed a large diurnal warming trend at LOTUS. The LOTUS 0.6 m temperature and satellite-derived SST values for this period are plotted in the upper panel of Fig. 1. The satellite-derived temperatures are slightly higher than the corresponding LOTUS temperatures with the difference being larger at night than during the day. The mean difference between satellite and LOTUS data for the eight values shown in Fig. 1 is less than 0.3°C with a standard deviation of 0.2°C, less than the standard deviation of 0.45°C obtained from the 39 clear images discussed earlier (of which these eight are a subset). The smaller deviation results from the relatively short period considered, during which meteorological conditions affecting atmospheric attenuation were stable. The day–night temperature differences (lower curve in Fig. 1) derived from the satellite data are in good agreement with the in situ measurements, with only slightly lower differences due to the larger temperature differences at night. Similar good agreement between the mooring and satellite data is found for all 22 selected days. Three observations are discussed in detail in section 6.

The largest diurnal warming event visible at LOTUS occurred on 26 July 1982 (Fig. 2c) with a maximum night–day temperature difference at 0.6 m depth of 3.2°C and a difference of 3.0°C at the times of the two satellite passes. Although a comparison at the mooring site between satellite and mooring data is not possible on this day because of small clouds centered on LO-

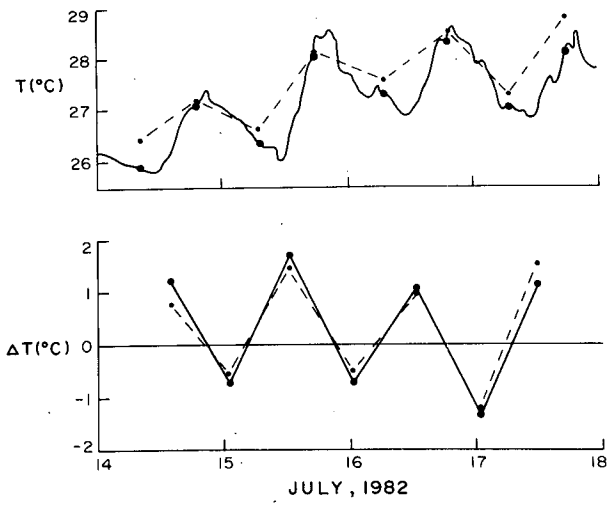

FIG. 1. SST at 34°N, 70°W for the period 14–18 July 1982 (upper curves) and the day–night temperature differences (lower curves) from satellite data (dashed line) and in situ measurements at 0.6 m depth (solid line). Time is GMT (subtract 0.21 for local solar). The dots on the upper curves represent temperatures at the time of the satellite pass.

TUS, contours of the differences between the day pass and the night pass, smoothed with a 3 × 3 median filter, show differences of 3.5°C in the vicinity of LOTUS, 17% higher than the mooring results. Of the remaining four days on which the mooring data showed warming of more than 2°C (Table 2), only two day-following night satellite pairs were cloud-free at LOTUS. These two pairs had satellite temperature differences approximately 30% higher than those derived from the mooring. Hence, for days with warming of more than 2°C, the warming sensed by satellite is about 20 to 30% higher than the thermal signal seen at 0.6 m depth.

For the western Sargasso Sea north of 29°N a maximum surface warming of 3.5°C over an area of 100-km diameter is often seen in the satellite data. Small areas showing SST differences of up to 4°C are found occasionally in satellite data, but the existence of 4°C temperature differences can not be verified with the in situ dataset used here.

5. Simulation of the LOTUS temperature measurements

We have simulated the upper ocean temperatures observed at LOTUS during the period 12–30 July 1982 using the one-dimensional model developed by Price et al. (1985; hereafter, PWP). The aim of these simulations is to test the model under the low wind speed and strong heating conditions that occurred during much of this period and to use the model to help describe the dynamics of the large-amplitude diurnal warming events observed in the LOTUS and satellite datasets.

In brief, the PWP model assumes that diurnal warming is a local response to solar insolation, surface heat loss, and wind-mixing (e.g., Niiler and Kraus, 1977). Insolation is absorbed within the water column but most strongly near the surface (details below). The absorbed heat can be mixed deeper into the water column by wind-mixing, which is parameterized as an adjustment to shear flow stability, and by free convective mixing, which occurs whenever there is heat loss from the sea surface. One result of these simulations is a diagnostic that shows which of these two mixing processes is dominant on a given day.

At most oceanic sites the local heat balance assumption inherent in one-dimensional models such as ours is grossly violated because of horizontal and vertical heat advection associated with low-frequency eddy motions (e.g., PWP; and to a much lesser extent, Davis et al., 1981). These advective effects can badly obscure the local response of the ocean to atmospheric forcing. We are fortunate here that the LOTUS temperature measurements show almost no advective effects during this period (note that aside from high-frequency fluctuations the 50 m temperature is nearly constant in Fig. 2) and are thus well suited for testing one-dimensional models.

a. Running the model

1) ESTIMATING THE SURFACE FLUXES

The model requires time series of the wind stress, τ, and of the surface heat flux, $Q = I + L$, which is the sum of insolation, I, and heat loss, L. Wind stress was estimated from the observed wind speeds, air temperatures and sea temperatures using the Large and Pond (1981) bulk aerodynamic method. The estimated wind stress magnitude varied substantially, from nearly zero on several occasions to as much as 0.25 N m^{-2} (Fig. 2b).

Insolation was directly measured by pyranometer (Fig. 2a). Heat loss, L, is the sum of infrared, sensible, and latent heat fluxes. The former was calculated from conventional radiation formulae (Kondratyev, 1969), by which cloud cover was estimated from observed insolation compared to the expected clear sky values (Tabata, 1964). Sensible heat flux was calculated from the observed wind speeds, air temperatures, and sea temperatures using the Large and Pond (1982) bulk formulae. Estimation of the latent heat flux requires some measure of the humidity. Because of the unreliable VAWR measurements of humidity, ship reports within 55 km of LOTUS were used to find the dry bulb/dew point spread. Outlying values resulting from either short-term variability or bad data were rejected. During July 1982 the average spread was found to be 4°C, which corresponds to a relative humidity of 75%. This constant value of humidity is used throughout the period 12–30 July 1982. Temporal variations about

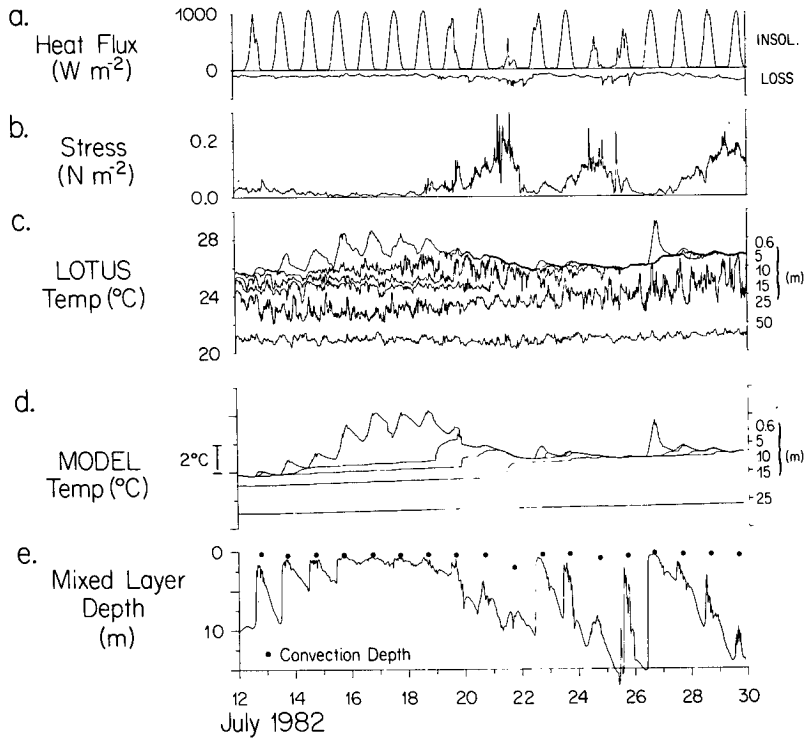

FIG. 2. Time series of surface fluxes and ocean temperatures for the LOTUS site. Time is GMT. (a) Measured insolation and heat loss estimated using the bulk formulae. (b) Wind stress magnitude. (c) Temperature at depths of 0.6, 5, 10, 15, 25 and 50 m measured at LOTUS. (d) Temperature at depths of 0.6, 5, 10, 15 and 25 m simulated by a numerical model. (e) Simulated mixed-layer depth (solid curve), and convection depth (dots, one per day).

this average will undoubtedly cause some unknown error in the estimated latent heat flux; however, as noted below, the days that produce the largest diurnal warming are characterized by very light wind, and thus by nearly vanishing sensible and latent heat flux. Under these conditions the total heat loss is dominated by the infrared loss, and the uncertainty in humidity is less worrisome than might otherwise be the case.

2) DOWNWARD IRRADIANCE

Solar insolation penetrates the water column to a depth that depends upon the optical properties of water. We do not have optical measurements of water surrounding LOTUS during this period and have therefore made the assumption that the LOTUS site in the mid-Sargasso Sea has type I (clear, open ocean) water, following Jerlov's (1968) classification. Paulson and Simpson (1977) have provided the parameters of a double exponential fit to Jerlov's type I water:

$$I(z) = I(0)[R \exp(-z/\beta_1) + (1 - R) \exp(-z/\beta_2)] \quad (2)$$

where $I(z)$ is the insolation as a function of depth, z, $R = 0.58$, $\beta_1 = 0.35$ m, and $\beta_2 = 23$ m. We use Eq. (2) to specify the downward irradiance in the model. Simpson and Dickey (1981) have noted that this double exponential form gives essentially the same results as several other more elaborate forms and is to be preferred here given the absence of optical measurements at the LOTUS site. (On days with very light winds, the model results are rather sensitive to β_1 as we discuss below.)

3) INTEGRATION

To resolve the strongly surface-trapped response expected on light wind days, the vertical grid interval was set to 0.2 m. Integration was begun from an initial condition estimated from the data at midnight on 11 July and continued at 15-min time steps until 30 July. The model-simulated temperature profile was sampled to produce time series at depths of 0.6, 5, 10, 15 and 25 m (Fig. 2d) for comparison with the buoy measurements.

b. Comparison with the LOTUS record

The LOTUS temperature data exhibit a high-frequency fluctuation at all depths below the surface mixed layer. At the 15 m level, these temperature fluctuations correspond to a vertical displacement of roughly 2 m rms. The disappearance of these high-

frequency fluctuations at a given level marks the arrival of the surface mixed layer at that depth. For example, the fluctuations disappear from the 5 m level during 19 and 20 July, coincident with an increase of the 5 m temperature to the 0.6 m temperature value. The same sequence occurs at the 10 m level on 21 July and rather gradually at the 15 m level from 22 to 25 July.

Aside from the high-frequency temperature fluctuations, the model-simulated temperature response is fairly similar to that observed at LOTUS. When the mixed layer arrives at a given level in the LOTUS record, it usually does so at about the same time in the simulated record. There are some differences. Most notably during the period 14–18 July, when the simulated 0.6 m temperature goes through about the same warming during the diurnal cycle, but then cools less at night. As a result, the simulated 0.6 m temperature trends upward somewhat more than does the observed 0.6 m temperature. This error is consistent with an underestimate of the surface heat loss of about 20 W m^{-2} (perhaps by underestimating the infrared heat loss).

c. *Day-to-day variability of the diurnal cycle*

It is most important that the model simulates well the large day-to-day variability of the diurnal surface warming observed at the 0.6 m LOTUS thermistor. This suggests that the model accounts for at least the dominant mixing and radiation processes that shape the diurnal cycle and, hence, that it is a useful guide for interpreting the differences between days.

1) MODERATE AND STRONG WINDS

On days with even moderate winds ($\tau \geq 0.03$ N m^{-2}), vertical mixing of heat (in the model) occurs primarily by wind mixing. For example, on 28 and 29 July heating was strong ($I > 1000$ W m^{-2}) but so was the wind stress ($\tau \geq 0.1$ N m^{-2}). As a result, the surface mixed layer remained at least 10 m thick on both days (inferred from the small temperature difference between 10 m and 0.6 m in the observed and simulated records), and thus the surface warming was fairly weak (<0.2°C). On these days, and more generally for the record as a whole, the day-to-day variations of diurnal surface warming are very strongly dependent on the day-to-day variations of the wind.

2) LIGHT WINDS

The days with the largest diurnal warming, >2°C, are invariably days with very light or almost no wind stress. Under these conditions wind mixing may become insignificant compared to convective mixing due to heat loss from the sea surface. Heat loss will cause mixing down to the convection depth C (Dalu and Purini, 1982), defined by

$$\frac{I(0) - I(C) + L}{C} = \left.\frac{\partial I}{\partial z}\right|_C. \tag{3}$$

At depth C, warming due to direct absorption of insolation is equal to the warming in the mixed layer above (see also Kraus and Rooth, 1961; Woods, 1980). The daily minimum convection depth has been computed from the estimated surface heat fluxes and plotted as one dot per day in Fig. 2e along with the simulated mixed layer depth.

On most days the mixed layer depth at noon is considerably greater than the convection depth, showing the dominance of wind mixing. However, on the days with the largest diurnal warming, 15–17 July and 26 July, the simulated mixed layer depth near local noon went to the convection depth (about 0.5 m), showing that wind mixing was of no significance on those days. That is, had the wind stress been literally zero there would have been no appreciable difference in the response of the model. It appears that largest diurnal warming events are governed by the simplest mixing dynamics involving only heat gain in the water column by insolation, heat loss from the surface mainly by infrared radiation, and free convective adjustment.

In the model simulations, the surface mixed layer is as shallow as 0.5 m on these days, which suggests that the 0.6 m temperature should be a fairly good measure of the surface temperature. The trapping depth, or mean-depth value of the diurnal warming (Price et al., 1985) is about 1.5 m, so that measurements made as shallow as 2 m depth would be expected to show a much weaker diurnal response (note that the 5 m LOTUS temperature shows no apparent diurnal warming on 14–18 July).

The convection depth and the surface warming are fairly sensitive to β_1, the extinction coefficient for longwave insolation [Eq. (2)], and to the heat loss, L. For the sensitivity of surface warming, the relation between ΔSST ($T_{day} - T_{night}$) and β_1 has been found from numerical experiment to be

$$\partial(\ln\Delta\text{SST})/\partial(\ln\beta_1) = -0.8,$$

and similarly the sensitivity to heat loss is

$$\partial(\ln\Delta\text{SST})/\partial(\ln L) = 0.7.$$

In studies such as this, the sea water optical properties and the heat loss (especially the infrared component) should be specified very carefully, certainly more precisely than was possible here, and preferably by direct observations.

6. Horizontal extent and pattern of warming

The satellite-derived SST fields (median-filtered on 7×7 pixel squares) for the night (0240 local time) and day (1406 local time) of 16 July 1982 are shown in Figs. 3 and 4, respectively. A cloud band from a meteorological front moving toward the south is seen in the north. In the night (Fig. 3) between 33° and 34°N and between 68° and 71°30′W, two areas warmer than the surrounding water may be seen (28°–29°C). These

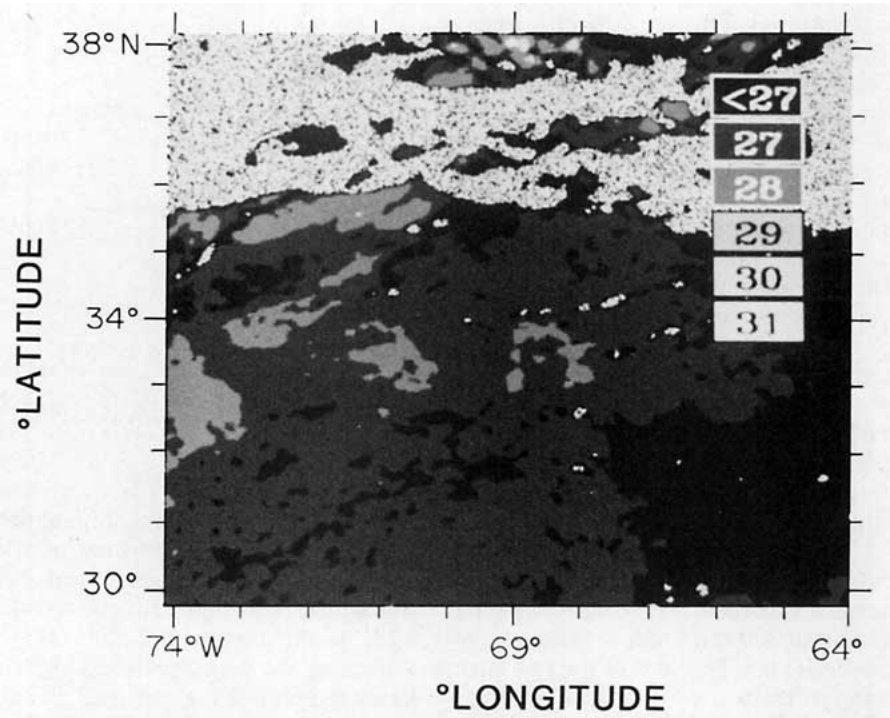

FIG. 3. Nighttime satellite-derived SST field for 16 July 1982 (0740 GMT; 0240 local time), smoothed with a 7 × 7 median filter. Clouds are stippled. Grey scale is in °C.

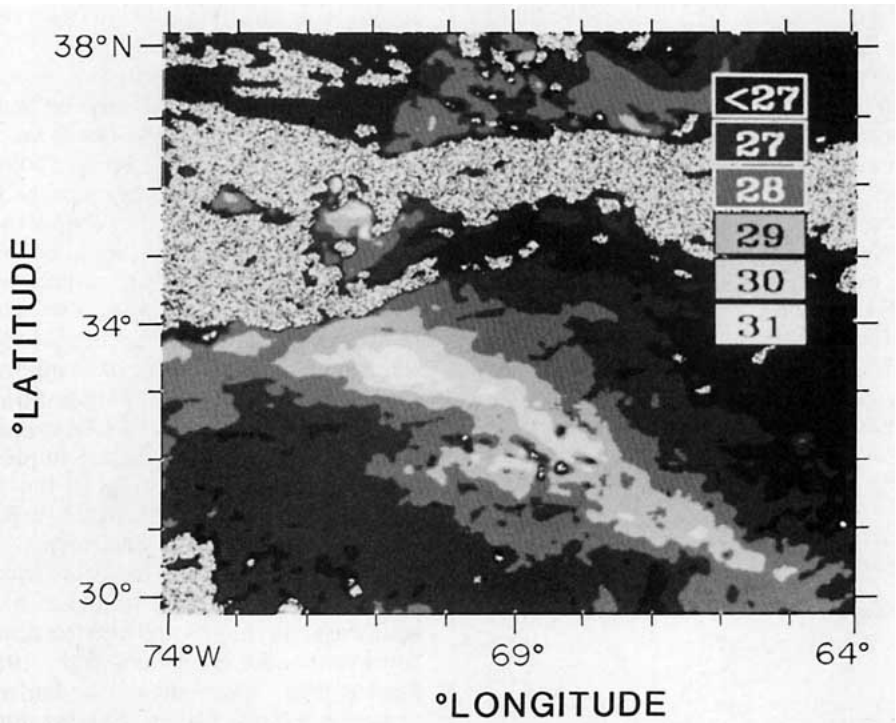

FIG. 4. Daytime satellite-derived SST field for 16 July 1982 (1906 GMT; 1406 local time), smoothed with a 7 × 7 median filter. Clouds are stippled. Grey scale is in °C.

result from diurnal warming of the previous day, where the heat gain in daytime was larger than the heat loss the following night. The area influenced by diurnal warming is readily visible in Fig. 4 as the long, narrow, relatively lighter region south of the clouds. Small, negative temperature anomalies (darker), for example between 31° and 32°30′N, 68° and 70°W, are thin clouds. The higher temperature north of the large clouds at 37°N is the Gulf Stream. In the northwestern Sargasso Sea, diurnal warming often appears in long, narrow regions with an east–west orientation. The 16 July warming event is typical of the other events observed in this study.

The region of diurnal warming was defined in this work by subtracting the night satellite pass from the day pass. The resulting image of day–night SST differences was smoothed with a 3 × 3 median filter to reduce noise and the influence of small clouds. Figure 5 gives the 1, 2, 3 and 4°C contours of warming digitized from the day–night differences of 16 July 1982. The region for which the warming exceeded 1°C is approximately 1500 km long and up to 300 km wide, with an area of approximately 300 000 km^2. The sum of the two large areas with warming in excess of 2°C is 130 000 km^2. The 3°C contours are split into 4 smaller areas while the 4°C contour encloses only a small area at 31°N, 66°20′W. The difference between the maximum daytime temperature and the minimum nighttime temperature might be even larger (Fig. 1), because the satellite does not pass exactly at the time of the maximum and minimum temperatures. The day–night temperature differences derived from the LOTUS data at times corresponding to satellite passes range from 40 to 95% of the maximum day–night difference on the same day, with a mean value of about 70%. Therefore, the amplitude of diurnal warming is underestimated by the satellite data; i.e., the area shown in Fig. 5 by the 1°C contour underestimates the area covered by diurnal warming in excess of 1°C. The same is true for the other contours, as well.

A 290-km SST section obtained from the median-filtered images for the night and day passes on 16 July 1982 is shown in Fig. 6. This section is oriented from southwest to northeast (32°36′N, 71°24′W to 34°36′N, 69°24′W) and passes through the LOTUS site. In the

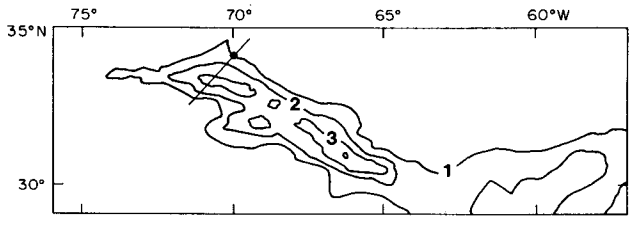

FIG. 5. Isolines of the day–night temperature difference in °C on 16 July 1982 from satellite data. The LOTUS position is shown as a dot. The line shows the section presented in Fig. 6.

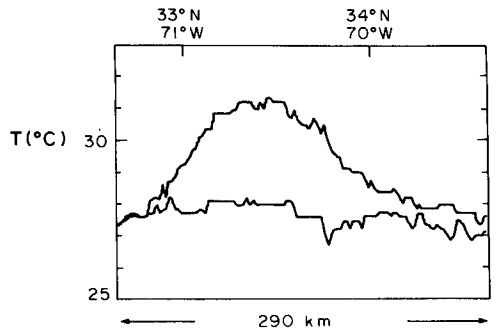

FIG. 6. Satellite-derived SST section for the night (0740 GMT; lower curve) and the day (1906 GMT; upper curve) of 16 July 1982 between 32°36′N, 71°24′W (left) and 34°36′N, 69°24′W (right).

southwest (left end) the night and day SST values are almost the same, while in the northeast the gradient of warming (upper curve) is weak, resulting in a large area with a day–night temperature difference of about 0.7°C to the northeast of the LOTUS position.

Because low wind speed and high insolation are necessary to obtain a large diurnal signal, the spatial contours of the region of warming on this day were transferred to the corresponding weather map (European Meteorological Bulletin, 1982) to determine if the area of apparent diurnal warming corresponds to such a scenario (Fig. 7). The time of the meteorological observations, 2400 GMT, is about 6 hours later than that of maximum warming. Wind observations from ships are presented as arrows.

The 1020 mb isoline in Fig. 7 of a large Azores–Bermuda high extends across the Sargasso Sea to the coast of the United States. The front north of 34°N in this weather map can be seen in Figs. 3 and 4 as the east–west cloud front. Since surface winds are nearly geostrophic over water, they follow the isobars closely, so the lowest wind speeds should be found in the center of the ridge of the 1020 mb contour. Ship observations of wind velocity show low wind velocities near the area of warming. The fit between contours of diurnal warming and those of the 1020 mb isobar is excellent. From this observation it is expected that the area of diurnal warming extends to the east and southeast. In most cases the diurnal signal found at the LOTUS mooring is caused by a ridge of the Azores–Bermuda high extending to the west, which explains the preferred east–west orientation of warming. On 18 July 1982 (Fig. 8), two days after the SST fields for Figs. 3 and 4, the cold front (solid triangles) had moved to the southeast with the warm front (solid semicircles) to the southwest and the Bermuda high is separated from the Azores high, which moved to the northeast with its center over Great Britain. This situation resulted in the Bermuda high having a southwest–northeast orientation, and the area of warming again fits the isobar very well.

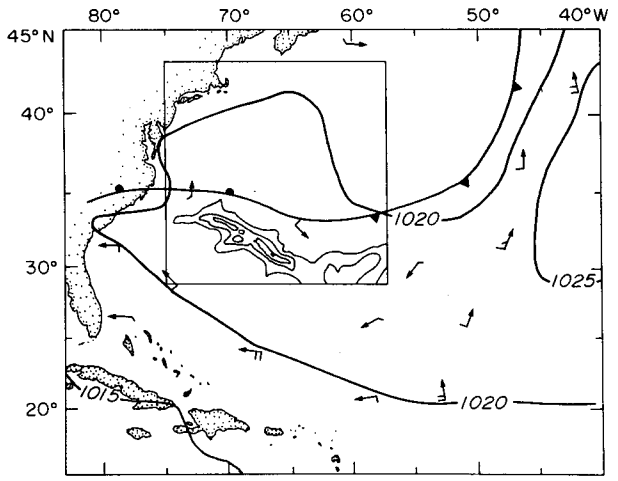

FIG. 7. Diurnal warming contours in isolines of 1°C (thin lines), surface pressure in millibars with 5 mb spacing (thick lines, labeled), fronts and wind observations for 16 July 1982. The closed box shows the area covered by the satellite. A short slanting stroke at the end of an arrow represents a wind speed of 2.5–7.5 kt (1 kt = 0.51 m s^{-1}); a perpendicular stroke indicates a speed of 7.5–12.5 kt; multiple strokes are summed.

The meteorology on 26 July, shown in Fig. 9, is different from that in Figs. 7 and 8. The center of the Atlantic high is located at 35°N, 40°W. The 1020 mb isobar is situated southeast of LOTUS, and a cloud band is connected to the cold front at the 1020 mb isobar. The spacing between the 1020 mb isobar and the 1015 mb isobar is very large. The 1015 mb isobar reaches the Mexican coast and the center of the east coast of the United States. Therefore, a large area of low wind speed is expected west of the cold front. Warming of more than 1°C is found between the front southeast of LOTUS and the coast of the United States. Large temperature differences of up to 3°C appear south of LOTUS and at LOTUS.

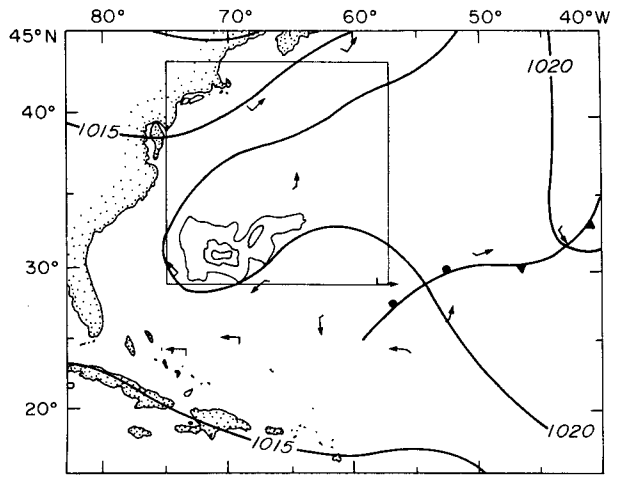

FIG. 8. As in Fig. 7 except for 18 July 1982.

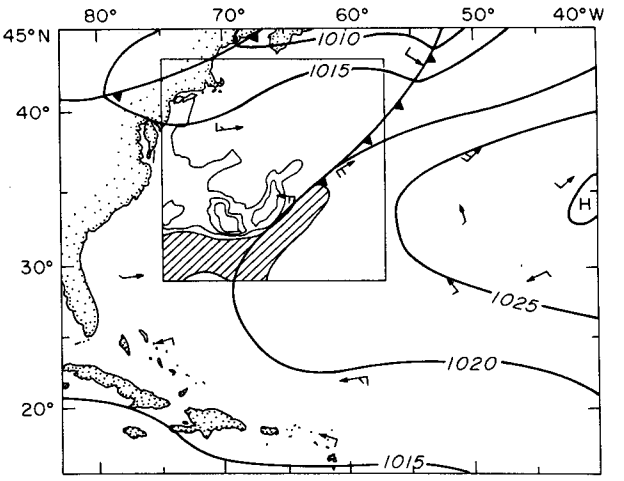

FIG. 9. As in Fig. 7 except for 26 July 1982. The shaded region represents the large clouds observed in the satellite data just south of the diurnal warming area.

All 22 day–night pairs investigated show a clear relation between large diurnal warming and low wind speeds with high insolation. For the area around LOTUS, these conditions exist for 18 of the 22 days associated with a westward-extended ridge of the Azores–Bermuda high. This gives low wind speeds in the center of the ridge and causes the frequent east–west extension of the warming area. This meteorological situation, however, is not essential for diurnal warming; it is necessary only to have low wind velocity and high insolation.

7. Conclusions and discussion

Near-surface temperature data from a two-year mooring were combined with coincident satellite-derived SST fields to investigate diurnal warming events in the open ocean. The comparison between these two datasets shows that, with careful screening for clouds, the satellite provides reliable SST measurements of diurnal warming. Furthermore, the diurnal warming observed at the mooring and by the satellite is well simulated by a one-dimensional model, suggesting that the conditions for a large response of the SST are high insolation and low wind speeds. Simulations of the largest events require only radiation absorption, radiative heat loss and free convective adjustment. From the satellite data it is seen that these diurnal warming patterns are of large horizontal extent, the area of warming of more than 1°C exceeding on occasion 300 000 km^2. Furthermore, these events are well correlated with synoptic pressure patterns. These large events have probably been underreported in the past because they are limited to depths between 1 and 2 m. Ship observations are usually taken deeper than 2 m and tend to miss the events. In this work it has been shown that satellite data is appropriate to study the extent of these phenomena.

The large diurnal SST signal suggests that in using satellite data to estimate long-term mean SST fluctuations, the local sun time of the satellite pass must be considered in the computations. Gruber and Krueger (1984), drawing on their observation that the day–night difference in outgoing longwave radiation changes significantly with the time of the satellite equatorial crossing, emphasize the importance of a continuous record of satellite data with the same equatorial crossing times for studies such as theirs. Similarly, long-term estimates in the mean SST field derived from satellite data are biased by the local sun time of the satellite pass. For example, the mean temperature for July 1982 calculated from the 0.6-m deep thermistor of the LOTUS mooring at 0200 local time (0700 GMT), the time of the NOAA-7 descending node, is 25.07°C, while at 1400 local time (1900 GMT), the time of the NOAA-7 ascending node, the monthly mean temperature is 25.47°C. This 0.4°C difference is further accentuated by the fact that the satellite observations are biased toward cloud-free observations; hence the daytime observations will be biased high by diurnal heating events such as those discussed in this paper when compared to the LOTUS mean values. This will tend to increase the day–night difference above the 0.4°C estimated from the LOTUS data. This is not to say that satellite-derived mean SST values should not be used for long-term studies, only that they should be corrected for these biases where possible.

Satellite-derived SSTs have been shown to provide reliable estimates of the magnitude and spatial extent of diurnal warming. A statistical analysis of such events based on satellite data in a larger area of the western North Atlantic has been performed by Cornillon and Stramma (1985). Also in progress is a comparison between forecasts of diurnal warming by an operational model and measurements from satellite data. From Sandwell and Agreen's (1984) estimated wind field, it follows that large diurnal warming should be expected over large areas of the world ocean. The United States Navy currently has an ocean thermal model functioning in real time at the United States Navy's Fleet Numerical Oceanography Center, in which diurnal temperature differences of more than 0.5°C in the world ocean are forecast (R. M. Clancy, personal communication, 1985). Comparison of the model predictions with satellite observations will provide a measure of the accuracy of the model while at the same time allowing an investigation of diurnal warming on the global scale.

Acknowledgments. This research has been supported by the Office of Naval Research through Contracts N00014-81-C-0062 and N00014-76-C-0197. The image processing software was developed by O. Brown, R. Evans, J. Brown and A. Li at the University of Miami with Office of Naval Research funding. The continuing support of the Miami group is gratefully acknowledged, as is the editorial assistance provided by J. Rahn. Finally we would like to thank R. Bernstein for the initial suggestion that the anomalous warming events might be attributed to diurnal warming.

REFERENCES

Briscoe, M. G., and R. A. Weller, 1984: Preliminary results from the Long Term Upper Ocean Study (LOTUS). *Dyn. Atmos. Oceans,* **8,** 243–265.

Bruce, J. G., and E. Firing, 1974: Temperature measurements in the upper 10 m with modified expendable bathythermograph probes. *J. Geophys. Res.,* **79,** 4110–4111.

Cornillon, P., and L. Stramma, 1985: The distribution of diurnal sea surface warming events in the western Sargasso Sea. *J. Geophys. Res.,* **90,** 11 811–11 816.

Dalu, G. A., and R. Purini, 1982: The diurnal thermocline due to buoyant convection. *Quart. J. Roy. Meteor. Soc.,* **108,** 929–935.

Davis, R. E., R. DeSzoeke, D. Halpern and P. Niiler, 1981: Variability in the upper ocean during MILE. Part I: The heat and momentum balances. *Deep-Sea Res.,* **28,** 1427–1451.

Deschamps, P. Y., and R. Frouin, 1984: Large diurnal heating of the sea surface observed by the HCMR experiment. *J. Phys. Oceanogr.,* **14,** 177–184.

Deser, C., R. A. Weller and M. G. Briscoe, 1983: Long Term Upper Ocean Study (LOTUS) at 34°N, 70°W: Meteorological sensors, data and heat fluxes for May–October 1982 (LOTUS-3 and LOTUS-4). Woods Hole Oceanogr. Inst. Tech. Rep. WHOI-83-32, 68 pp.

European Meteorological Bulletin, 1982: *Deutscher Wetterdienst Zentralamt,* 6050 Offenbach, **7,** diurnal maps.

Grassl, H., 1976: The dependence of the measured cool skin of the ocean on wind stress and total heat flux. *Bound.-Layer Meteor.,* **10,** 465–474.

Gruber, A., and A. F. Krueger, 1984: The status of the NOAA outgoing longwave radiation data set. *Bull. Amer. Meteor. Soc.* **65,** 958–962.

Halpern, D., and R. K. Reed, 1976: Heat budget of the upper ocean under light winds. *J. Phys. Oceanogr.,* **6,** 972–975.

Jerlov, N. G., 1968: *Optical Oceanography.,* Elsevier, 194 pp.

Kaiser, J. A. C., 1978: Heat balance of the upper ocean under light winds. *J. Phys. Oceanogr.,* **8,** 1–12.

Kondratyev, K. Ya., 1969: *Radiation in the Atmosphere.* Academic Press, 571–573.

Kraus, E. B., and C. Rooth, 1961: Temperature and steady state vertical heat flux in the ocean surface layers. *Tellus,* **13,** 231–238.

Large, W. G., and S. Pond, 1981: Open ocean momentum flux measurements in moderate to strong winds. *J. Phys. Oceanogr.,* **11,** 324–336.

——, and ——, 1982: Sensible and latent heat flux measurements over the ocean. *J. Phys. Oceanogr.,* **12,** 464–482.

Lynn, R. J., and J. Svejkovsky, 1984: Remotely sensed sea surface variability off California during a "Santa Ana" clearing. *J. Geophys. Res.,* **89,** 8151–8162.

McClain, E. P., W. G. Pichel, C. C. Walton, Z. Ahmad and J. Sutton, 1983: Multi-channel improvements to satellite derived global sea surface temperatures. *Adv. Space Res.,* **2,** 43–47.

McMillin, L. M., and D. S. Crosby, 1984: Theory and validation of the multiple window sea surface temperature technique. *J. Geophys Res.,* **89,** 3655–3661.

Niiler, P. P., and E. B. Kraus, 1977: One-dimensional models of the upper ocean. *Modelling and Prediction of the Upper Layers of the Ocean.* E. B. Kraus, Ed., Pergamon, 285 pp.

NOAA/NESDIS, 1982: Coefficients presented at the 32nd SST Research Panel Meeting. National Environmental Satellite, Data,

and Information Service (NESDIS), National Oceanic and Atmospheric Administration (NOAA), Suitland, MD.

Paulson, C. A., and J. J. Simpson, 1977: Irradiance measurements in the upper ocean. *J. Phys. Oceanogr.*, **7**, 952–956.

——, and ——, 1981: The temperature differences across the cool skin of the ocean. *J. Geophys. Res.*, **86**, 11044–11054.

Payne, R. E., 1974: A buoy-mounted meteorological recording package. Woods Hole Oceanogr. Inst. Tech. Rep. WHOI-74-40, 31 pp.

Price, J. F., R. A. Weller and R. Pinkel, 1986: Diurnal cycling: Observations and models of the upper ocean response to diurnal heating, cooling, and wind mixing. *J. Geophys. Res.*, **91** (in press).

Sandwell, D. T., and R. W. Agreen, 1984: Seasonal variation in wind speed and sea state from global satellite measurements. *J. Geophys. Res.*, **89**, 2041–2051.

Schwalb, A., 1978: The TIROS-N/NOAA A-G satellite series. NOAA Tech. Memo. NESS 95, U.S. Govt. Printing Office, Washington, DC, 75 pp.

Simpson, J. J., and T. D. Dickey, 1981: Alternative parameterizations of downward irradiance and their dynamical significance. *J. Phys. Oceanogr.*, **11**, 876–882.

Stommel, H., K. Saunders, W. Simmons and J. Cooper, 1969: Observations of the diurnal thermocline. *Deep-Sea Res.*, **16**(Suppl.), 269–284.

Tabata, S., 1964: Insolation in relation to cloud amount and sun's altitude. *Studies on Oceanography*, K. Yoshida, Ed., University of Tokyo Press, 202–210.

Woods, J. D., 1980: Diurnal and seasonal variation of convection in the wind-mixed layer of the ocean. *Quart. J. Roy. Meteor. Soc.*, **106**, 379–394.